REVIEW ARTICLE

Correlation of Electrocardiogram and Regional Cardiac Magnetic Resonance Imaging Findings in ST-Elevation Myocardial Infarction: A Literature Review

Irina Rinta-Kiikka, M.D., Ph.D.,* Suvi Tuohinen, M.D.,† Pertti Ryymin, Ph.D.,* Petteri Kosonen, M.D.,‡ Heini Huhtala, M.Sc.,§ Anton Gorgels, M.D., Ph.D.,¶ Antonio Bayés de Luna, M.D., Ph.D.,‖ and Kjell Nikus, M.D., Ph.D.†

*From the *Department of Clinical Radiology, Tampere University Hospital, Finland; †Heart Hospital, Tampere University Hospital and Tampere University, Medical School, Finland; ‡Department of Internal Medicine, Savonlinna Central Hospital, Finland; §School of Health Sciences, University of Tampere, Tampere, Finland; ¶Maastricht University Medical Centre, Maastricht, the Netherlands; and ‖Institut Català Ciències Cardiovasculars, Barcelona, Spain*

Background: Patients with acute ST-elevation myocardial infarction (STEMI) benefit substantially from emergent coronary reperfusion. The principal mechanism is to open the occluded coronary artery to minimize myocardial injury. Thus the size of the area at risk is a critical determinant of the patient outcome, although other factors, such as reperfusion injury, have major impact on the final infarct size. Acute coronary occlusion almost immediately induces metabolic changes within the myocardium, which can be assessed with both the electrocardiogram (ECG) and cardiac magnetic resonance (CMR) imaging.

Methods: The 12-lead ECG is the principal diagnostic method to detect and risk-stratify acute STEMI. However, to achieve a correct diagnosis, it is paramount to compare different ECG parameters with golden standards in imaging, such as CMR. In this review, we discuss aspects of ECG and CMR in the assessment of acute regional ischemic changes in the myocardium using the 17 segment model of the left ventricle presented by American Heart Association (AHA), and their relation to coronary artery anatomy.

Results: Using the 17 segment model of AHA, the segments 12 and 16 remain controversial. There is an important overlap in myocardial blood supply at the antero-lateral region between LAD and LCx territories concerning these two segments.

Conclusion: No all-encompassing correlation can be found between ECG and CMR findings in acute ischemia with respect to coronary anatomy.

Ann Noninvasive Electrocardiol 2014;19(6):509–523

ECG; cardiac MR; acute myocardial infarction; coronary artery territories

Cardiac magnetic resonance (CMR) imaging is considered the gold standard in the assessment of cardiac function and structure.[1] CMR imaging has emerged as a powerful noninvasive technique for the evaluation of myocardial function, perfusion, and viability in a single study without the need for radioactive tracer administration, which is a distinct attribute of the method.[2,3] CMR imaging has been shown to have a higher spatial resolution when compared to nuclear perfusion imaging techniques.[4] Late gadolinium enhancement (LGE) CMR after administration of Gadolinium-chelated contrast agents is a well-established method for assessing focal fibrosis of

Address for correspondence: Irina Rinta-Kiikka, M.D., Ph.D., Consultant Radiologist, Department of Clinical Radiology, Tampere University Hospital, P.O. Box 2000, FIN-33521, Tampere, Finland. Fax: +358331165586; E-mail: irina.rinta-kiikka@pshp.fi

Financial Support: This study was financially supported by the Competitive State Research Financing of the Expert Responsibility area of Tampere University Hospital, grant number 9F174.

DOI:10.1111/anec.12210

the myocardium in myocardial infarction (MI).[5] The delayed-enhancement technique also has high sensitivity for the identification of acute MI (AMI)[6] with the ability to detect as little as 1 g of irreversibly damaged tissue.[7] Moreover, abnormalities of left ventricular (LV) wall dynamics are sensitive markers of myocardial ischemia.[8] The exact measurement of infarct size, which is possible by CMR, may provide valuable information on ventricular remodeling, arrhythmic potential, and prognosis and is a commonly used surrogate endpoint for the evaluation of new MI therapies.[9]

The most widely used clinical method to diagnose acute coronary occlusion is by observing ST deviation on the electrocardiogram (ECG).[10] After acute epicardial coronary artery occlusion, and after the appearance in the ECG of tall and peaked T waves, ST elevation, representing transmural ischemia, appears if the artery remains occluded.[11] Methods based on the distribution of ST changes have proven to be useful for localizing the myocardial area at risk (AAR) during coronary occlusion.[12–14] Based on anatomical studies, a relationship between the location of infarcted areas and Q waves in the ECG was accepted and, with minor modifications, implemented in scientific statements and textbooks.

The 12-lead ECG is a cheap and universally available diagnostic method to detect and risk-stratify AMI. However, as with many other diagnostic methods, the ECG has its limitations potentially leading to false diagnostic and prognostic conclusions. Investigators originally used experimental and autopsy studies as the reference method to determine the location and to estimate the size of MIs based on the ECG. Later on, ECG findings were compared with coronary angiography, echocardiography, and nuclear imaging. CMR imaging has now emerged as the golden standard with respect to size and location of MI.

Our aim is to give an overview of the literature regarding ECG and CMR correlation in acute ST-elevation MI (STEMI), with the emphasis on the detection of regional changes. Because the coronary artery circulation is critical in determining the character of both ECG and CMR changes in AMI, coronary anatomic aspects will be covered.

Coronary Artery Anatomy

The coronary artery circulation is composed of two principal coronary arteries, the left (LCA) and the right coronary artery (RCA). Variations in the branching patterns are extremely common in the human heart. According to the Bypass Angioplasty Revascularization Investigators (BARI) classification, the RCA is predominant in approximately 85% of individuals, providing the posterior descending (PD; i.e., posterior interventricular) branch and at least one posterolateral (PL) branch.[15] In 7–8% of individuals, the coronary circulation is left dominant; the PL, the PD, and the atrioventricular nodal branches are all supplied by the terminal portion of the left circumflex coronary artery (LCx). In another 7–8% of hearts, there is a codominant or balanced system, in which the RCA gives rise to the PD branch, and the LCx gives rise to all the PL branches. The left anterior descending (LAD) and the LCx arteries are direct continuations of the left main trunk. One or more left diagonal (LD) and approximately 10 septal branches arise from the LAD, while left obtuse marginal branches arise from the LCx. In approximately one-third of individuals, the left main coronary artery trifurcates; the intermediate branch comes off between the LAD and the LCx.

In a normal heart with right-dominant coronary circulation, the LCA supplies approximately 5 times more blood to the LV than the RCA; the corresponding number for the LAD and LCx is approximately 3.5 and 1.5 times, respectively.[16] In the Alberta Provincial Project for Outcome Assessment in Coronary Heart Disease (APPROACH) scoring system, the LV is divided into regions according to pathological studies in humans evaluating the relative proportion of the myocardium perfused by each coronary artery.[17] Considering the location (proximal, mid, or distal) of the culprit lesion, investigators created a template that calculates the jeopardized myocardium for a given site occlusion, taken into consideration coronary artery dominance.[18]

Association between Segmental MI ECG Signs of Necrosis

Monumental work in the 1930s and 1940s established the theoretical and empirical basis for the association between myocardial necrosis and ECG findings.[19,20] Based on pathological correlation, a relationship between the location of infarcted areas and Q waves was accepted and, with minor modifications, implemented in scientific statements and textbooks.[21] According

to these studies, Q waves correspond to the following myocardial segments: leads V_1-V_2 to the septal wall, leads V_3-V_4 to the anterior wall, leads I and aVL to the lateral wall, and leads II, III, and aVF to the inferior wall. The mirror pattern (high R wave) in leads V_1-V_2 was traditionally considered as corresponding to the basal part of the inferoposterior wall (named true posterior MI).[22] The traditional view was that Q waves represent transmural MI, while subendocardial MI is reflected by ECG changes other than Q waves. Later on, autopsy studies showed that about half of subendocardial MIs generated pathological Q waves, while about half of transmural MIs did not.[23] The terms Q-wave and non-Q-wave MI replaced the former designations. CMR studies have shown that the Q-wave/non-Q-wave distinction is determined rather by the total size rather than by the transmural extent of the underlying MI.[24]

Already in the 1930s, studies showed different premortal ECG patterns depending on which epicardial coronary artery had thrombotic occlusion on autopsy.[25] With the introduction of coronary angiography, it became possible to correlate ECG findings of myocardial necrosis with this new technique.[26] Reperfusion therapy, initially by intracoronary thrombolysis in the 1980s, resulted in a clear need to improve ECG diagnostics to be able to predict the culprit artery and the estimated size of the AAR by observing changes from the acute occlusive phase—the ST segment and the T wave. Since then, many investigators have presented ECG algorithms to predict the culprit artery and the level of occlusion within the culprit artery based on the distribution of ST deviations.

The 17-Segment Model

Nuclear cardiology, echocardiography, cardiac computed tomography (CT), positron emission CT, and CMR are important imaging modalities of the myocardium and the adjacent cavity. The American Heart Association (AHA) writing group on Myocardial Segmentation and Registration for Cardiac Imaging aimed at harmonizing the imaging modalities with respect to the display of the ventricular segments.[27] Based on autopsy studies, the group presented a 17-segment model of the left ventricle (LV) for the visual interpretation of regional abnormalities. According to the statement paper, the model creates a distribution of 35%, 35%, and 30% for the basal, midcavity, and apical thirds of the heart. The authors also assigned individual LV segments to specific coronary artery territories (Fig. 1); segments 3, 4, 9, 10, and 15 were assigned to the dominant RCA, segments 5, 6, 11, 12, and 16 to the LCx, and segments 1, 2, 7, 8, 13, 14, and 17 to the LAD.

Temporal Aspects of AMI and Its Relation to CMR Imaging

In acute coronary artery occlusion, biomechanical and functional abnormalities begin immediately after the onset of ischemia. There is an immediate loss of contractility during the first minute, and in about half an hour loss of viability develops (Fig. 2). Initially, myocardial perfusion decreases leading to diminished tissue oxygenation, repolarization abnormalities, diastolic and systolic dysfunction, edema, and finally tissue necrosis. The infarct progresses like a wavefront from the endo- to the epicardium.[28] Progression to final necrosis takes 2–4 hours or longer, depending on factors like collateral circulation, persistent or intermittent coronary arterial occlusion, sensitivity of myocytes to ischemia, preconditioning, and individual demand for myocardial oxygen and nutrients.[29] In this cascade myocardial edema can occur in 30 minutes and progress to completely irreversible injury within 6–12 hours. This creates a window of opportunity, during which prompt reperfusion therapy may salvage myocardial tissue, which is still at risk of infarction. The progression of MI is a dynamic process, and this is why the timing between the acute event and evaluation of scar is paramount. The typical techniques used in CMR imaging are shown in Table 1 together with the underlying pathophysiology.

Technical and Clinical Aspects of CMR Imaging in AMI

Edema Imaging

Acutely infarcted myocardium contains increased amounts of free water as a natural consequence of AMI, including both irreversibly damaged and potentially salvageable myocardium.[30] Edema is visible in T_2-weighted images as bright areas in otherwise dark myocardium. In AMI patients, bright myocardium on T_2-weighted imaging reflects the myocardium at risk.[31] Edema changes are most evident in the acute or subacute phase

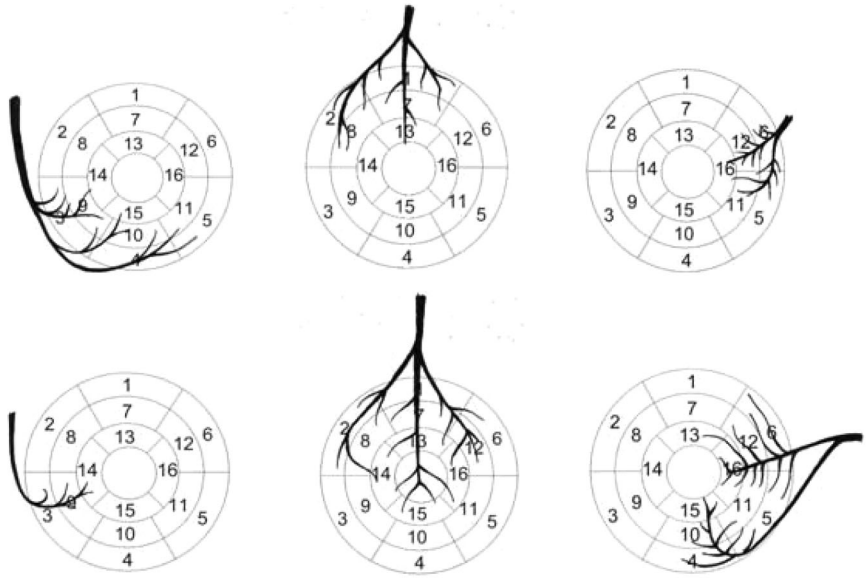

Figure 1. Coronary artery distribution in right (upper row) and left (lower row) dominance. The right coronary artery is shown to the left, the left anterior ascending in the middle, and the left circumflex artery to the right.

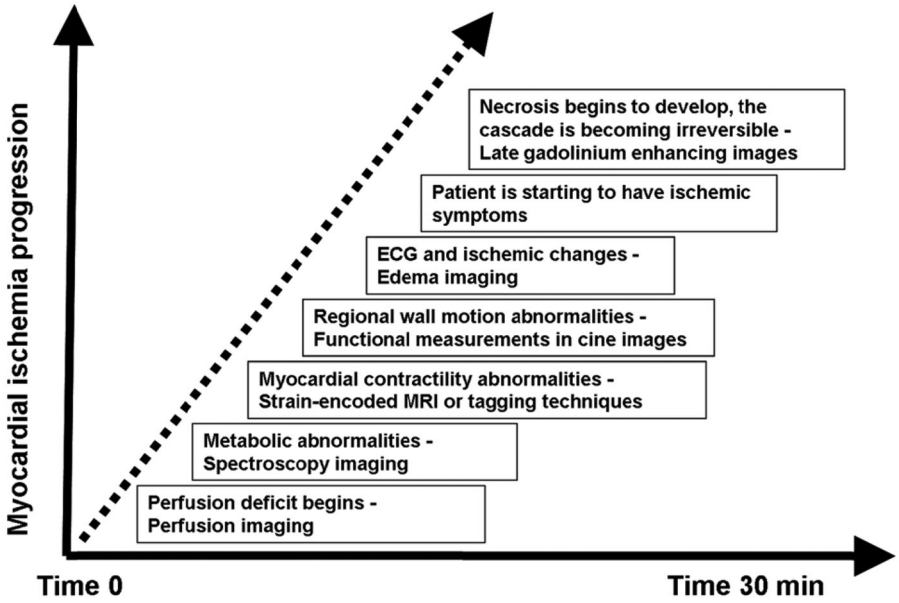

Figure 2. The ischemic cascade in the acute phase.

at least up to 1 week after the acute event,[30,32] after which they slowly fade away during the course of infarct healing with scar formation and resorption of infarct-related myocardial edema and inflammation.[30,33] T_2-weighted edema imaging can thus be used in differentiating between recent and healed MI.[31,34]

Late Gadolinium Enhancement

Mc Namara et al. introduced the basic principle of using gadolinium enhancement.[35] With the combination of the inversion recovery technique described by Simonetti et al.,[36] it became possible to maximize the contrast between viable and

Table 1. The Basic Sequences Used in Myocardial Infarction CMR Imaging

Sequence	Pathophysiology
T_2-weighted imaging	Myocardial edema, area at risk
Kine imaging, tagging techniques	Regional contractile and global ventricular function
Perfusion imaging, early gadolinium enhancement	Myocardial perfusion, microvascular obstruction
Late gadolinium enhancement	Infarct size, transmurality, persistent microvascular obstruction

infarcted myocardium. After gadolinium contrast administration, the enhancement reflects mainly irreversibly damaged tissue. Technically the best time window for infarct imaging is between 10 and 25 minutes postcontrast administration. If the acquisition is performed too early, LGE can lead to overestimation of the MI size.[37,38] There is significant decrease in the total extent of LGE between day 1 and day 7 post-MI.[39–41] CMR can be used in assessing MI size up to 1 week after the acute ischemic event. With time, the size of the infarct decreases as a result of resolution of tissue edema and gradual contraction of the resultant scar tissue by as much as 25% over a period of 4–8 weeks.[42]

Myocardial T1 Mapping and Extracellular Volume (ECV) Fraction

It is obvious that late gadolinium enhancement imaging provides crucial diagnostic and prognostic information in MI.[43,44] Nonetheless, LGE is a qualitative, not a quantitative diagnostic method. Previous canine CMR studies have shown alteration of the T1 time with fibrosis, which correlated with myocardial collagen content.[45] The T1 values can be encoded in each pixel, and a parametric map (T1-map) can be provided.[46] T1 measures permit noninvasive detection of biologically and pathologically important processes related to excess water in edema, protein deposition, and other T1 altering substances such as lipid or iron in hemorrhage.[46–50]

The ECV technique is sensitive to the distribution of the LV myocardium into its cellular and extracellular interstitial compartments.[47] Alterations in these compartments occurring from different physiologic and pathophysiologic biologic processes leading to fibrotic changes can be more easily detected with ECV than with LGE.[51] This is true especially with the changes resulting from pathologies other than MI, where the differences between the normal and affected myocardium are less distinct.[47,51–53] Therefore, the more widespread clinical use of these tissue characterization techniques requires further exploration.

Microvascular Obstruction (MVO) and Intramyocardial Hemorrhage (IMH)

Despite the beneficial effects of reperfusion, the process of cell death may continue during the first hours of reperfusion, a phenomenon called myocardial reperfusion injury. It is the consequence of clogging of the small myocardial arterioles with embolic debris, acute inflammation, platelet aggregation, and vasospasm.[54] According to Moens et al., reperfusion injury, with MVO as its main feature, has been detected in about 30% of patients.[55] The role of the 12-lead ECG for the assessment of MVO after PCI is not a topic to be discussed here, but it was recently covered in another review article.[56]

Early contrast-enhanced CMR can reliably demonstrate the presence and extent of MVO after reperfused AMI.[54] In addition, on LGE images MVO is seen as a central or subendocardial, hypointense, dark region within the enhanced bright area of infarcted myocardium. MVO progresses in size during the first 48 hours,[57] after which microvascular damage most likely stabilizes.[58] In one study of acutely revascularized MI patients, late MVO proved the most powerful predictor of global and regional functional recovery, even compared with transmural extent of MI.[59]

Besides MVO, IMH is considered another important feature of reperfusion injury; it is a consequence of blood extravasation through damaged endothelium.[60] IMH has been assessed by using different T_2-weighted imaging techniques.[61,62] Both MVO and IMH have been associated with adverse prognosis, adverse LV remodeling, and diminished recovery of LV function independently of infarct size.[63,64] CMR enables noninvasive evaluation of both MVO and IMH.

Left Ventricular Wall Motion Analysis by CMR

Following reperfused AMI, the LV undergoes structural alterations both within and outside of the area of infarction, referred to as LV remodeling. Ischemic regional remodeling starts soon after the onset of myocardial necrosis and progresses over time to extensive architectural changes of the whole ventricle.[65] The pathophysiology of the remodeling process is complex with multiple ultrastructural, metabolic, and neurally mediated processes occurring in infarcted and remote myocardium.[66] LGE detected in the infarct zone within 24 hours after primary PCI is an independent predictor of impaired LV systolic thickening and remodeling.[67] On the other hand, contractile function improvement has been reported to occur as a result of successful reperfusion.[68,69]

CMR is well suitable for the assessment of wall contraction patterns thanks to its capability for volumetric evaluation, and the ability to detect wall motion abnormalities even in regions inaccessible to echocardiography. In addition, CMR is less operator dependent than biplane echo.[70]

CMR using cine sequences is already considered the standard of reference for measurement of ventricular volume and various parameters of global ventricular function, such as ejection fraction (EF) and ventricular mass.[71] The cine-CMR technique allows accurate delineation of the endocardium and epicardium and offers a reproducible assessment of regional LV wall thickening.[72]

Masci et al. developed a CMR method to compare global and regional functional parameters.[73] One week and 4 months after MI, overall LV functional improvement matched with improvements in regional function of the infarcted region. In contrast, use of the 17-segment approach failed to depict significant differences over time in the infarcted myocardium, indicating that myocardial segments might contain a mixture of viable and nonviable myocardium, making accurate interpretation difficult.[73]

Masci et al. reported that improvement in global LV function matched with an improvement in systolic wall motion (SWM) but not with systolic wall thickening (SWT) in the infarcted myocardium.[73] This has been explained by the hypothesis that functional recovery of less-damaged outer myocardial layers may improve the myocardial wall motion leading to improved regional EF without substantial improvement in SWT.[74] According to Nowosielski et al., SWT <30% indicates an infarct size that affects LV function with correlation to the LV ejection fraction.[70] They also found a highly significant difference in SWT between segments with no LGE and those with transmural LGE of >50%, but pointed out that any infarcted segment is associated with some wall motion abnormality.[70] Therefore MI has a certain influence on the contractile function of the LV, not necessarily resulting in impaired ventricular function or clinical deterioration.

LV wall motion, thickening, and strain can be measured also by using the myocardial tagging technique,[75,76] which is performed with cine MR imaging by applying a special radio-frequency prepulse immediately following detection of R wave on the ECG tracing.[77] Myocardial tagging allows the determination and quantification of LV wall thickening of specific myocardial segments.[78,79]

Myocardial strain imaging provides a more accurate assessment of LV function, including circumferential and longitudinal contraction, compared with thickening analysis, which only shows cardiac motion in the radial direction.[80,81] Segmental strain analysis can be performed with CMR using myocardial tissue tagging with harmonic phase imaging, but has not yet become clinical routine.

Area at Risk

The AAR represents the amount of myocardium that is hypoperfused during coronary occlusion. Salvaged myocardium is defined as the AAR subtracted by the final infarct size and has an important role in estimating the therapeutic efficacy. Friedrich et al. concluded that the distinction between the areas with edema and LGE can be used as an estimate of AAR.[82] They stated that the areas with T_2 edema were invariably transmural and subsequently larger than the regions of LGE. The difference between them thought to most likely represent myocardial salvage.[82] This finding has also been supported with previous canine studies.[83]

The role of edema and AAR imaging with T_2-weighted technique has been studied a lot. Taking into account the wavefront character of irreversible ischemic injury, beginning from the endocardium and progressing to the epicardium, affects the potential for recovery of the myocardium after an ischemic episode. Different

myocardial layers have a different risk potential for ischemic damage. Histopathologic characterization of salvaged myocardium has shown that the subepicardial zone develops cellular necrosis less frequently than the subendocardial core of the infarction.[28] The fact that patients with aborted MI have more subendocardial and less transmural infarction by CMR provides imaging evidence for the concept of the wavefront phenomenon.[84] Taking these aspects into account, Ortiz-Perez et al. showed that CMR infarct endocardial surface area (ESA) measured within a week after primary PCI in STEMI patients correlated with the angiographically determined AAR.[18]

The use of T_2-weighted images in determining the AAR has its limitations.[85] In a review article, Arai et al. discussed the role of T_2-weighted MR imaging in the assessment of the AAR in patients with AMI.[86] More recent study findings, which have evaluated aspects of gadolinium kinetics, indicate that early gadolinium-enhanced images represent the AAR while LGE images correlate with the size of the MI.[86–88]

Also noncontrast T1 mapping technique has given promising results in revealing the AAR in acute coronary syndromes when combined in a clinical scan protocol.[59,89,90]

The Aldrich score is based on the total amount of ST deviation on admission and has been used as an ECG-based estimate of AAR.[91] In 78 reperfused STEMI patients, CMR methods (T_2-weighted hyperintensity and LGE ESA) were better than ECG methods (Aldrich score) for measuring AAR.[92] The authors speculated that the poor performance of the Aldrich score in estimating AAR might be explained by the dynamic nature of ST deviations in acute myocardial ischemia. The Anderson–Wilkins acuteness score was developed to enable assessment of acuteness of myocardial ischemia from the 12-lead ECG, and studies have indicated that it may be associated with salvageable myocardium.[93,94] A recent study of 38 patients treated with primary PCI, in which SPECT and CMR imaging were used to determine AAR and final infarct size, showed a moderate correlation between the acuteness score and salvageable myocardium in patients with acute RCA occlusion but not in patients with LAD occlusion. At present, there is no clear consensus regarding the preferred ECG method to estimate AAR.

Correspondence between Left Ventricular 17 Myocardial Segments and Coronary Artery Occlusion

Segmental analysis of myocardial perfusion studies is based on certain assumptions concerning coronary anatomy. The AHA working group that recommended the 17-segment model in LV imaging mentioned the tremendous variability in the coronary artery blood supply to myocardial segments, but the model was believed to be appropriate for assigning individual segments to specific coronary artery territories. Pereztol-Valdés et al. analyzed the correspondence of the 17 LV segments with each of the three major epicardial coronary arteries by myocardial perfusion single-photon emission CT (SPECT) studies during elective percutaneous coronary intervention (PCI) in 50 patients.[95] The study showed that the most specific segments (anterior, anteroseptal, and all apical segments except the inferoseptal) corresponded to the LAD, and the basal anterolateral segment (segment 6) to the LCx, while no segment could be exclusively attributed to the RCA. Eight segments were not attributed to a single coronary artery. In the working group paper, the inferior segments (4, 10, and 15) were attributed to the RCA, but in the study by Pereztol-Valdés et al., all patients with LCx disease had involvement of the inferior segments.[95] These observations most probably reflect the great variability in blood supply to the inferior and lateral wall.

In 2007, Ortiz-Perez et al. reported preliminary observations regarding the association between the anatomy of the coronary arteries and LGE localization in CMR.[18] In a subsequent study they reported on the correspondence between the 17-segment model and coronary artery anatomy with contrast-enhanced CMR imaging in 93 patients flowing AMI treated with primary PCI.[96] They found that four segments (2,7,8,and13) were 100% specific for LAD occlusion, while no segments were 100% specific for LCx or RCA occlusion. In a per-segment analysis, 23% of segments with LGE were found to differ from the coronary distribution empirically assigned to the 17-segment model. Misassignment of myocardial segments because of a deviation of true coronary anatomy from the standard model could alter the identification of the involved coronary vessel or the location of the

culprit lesion.[97] The agreement was remarkably low for the midanterolateral (segment 12) and apical lateral (segment 16) empirically attributed to the LCx—for all these segments, the culprit lesion was in the LAD.

In another study, where CMR images were coupled with noninvasive CT coronary angiography, the authors found the maximal discordance between the 17-segment model and CMR in segments 12,15, and 16, which were supplied by the LAD in most cases.[98] In this latter study, only 4 of 26 patients were found to agree with the model in all segments; on average, in a per-patient analysis there were differences in approximately three segments. LCx segments were most often discordant (35%), with the majority of the segments attributed to this artery being located within the LAD distribution. In fact, the Bayés de Luna group has demonstrated that myocardial injury caused by occlusion of the first diagonal branch involves part of segments 7 and 13 of the anterior wall, but also 12 and 16 of the lateral wall resulting in Q waves in lead aVL and often also in lead I. Accordingly, this type of MI represents an MI of the anterior/midanterior region, not of the basal lateral (LCx occlusion) or high lateral.[99,100] By level, apical segments were found to differ most often (26%), especially segments 15 and 16. Previous observations indicated the greatest variability with segment 17, but Setser et al. found this segment to agree better in their study.[27,98]

The LV apical area is more or less supplied by the LAD, portraying the large amount of myocardium supplied by this artery. Javadi et al. studied the coronary artery territories in perfusion images using PET/CT hybrid analysis.[97] They agreed with the observations by Pereztol-Valdés and Ortìz-Pérez that the standard assignment of vascular territories proposed by the AHA 17-segment model is frequently inaccurate.[95,96] However, the division by Cerqueira et al. into four walls and 17 segments is easy to understand and probably corresponds to a true anatomic correlation. They also reached promising results with CTA-derived imaging. Donato et al. performed an ex vivo study of cadaveric hearts using multidetector CT.[101] They showed that the LAD territory was larger than the AHA-proposed 17-segment model.[101] No specific segment could exclusively be attributed to the RCA or the LCx.[101] However, although segment 12 belonged to the LAD territory, the LAD and the LCx contributed almost equally to the blood supply of segment 16. Segment 12 corresponds to the lateral wall and due to many anatomic differences of coronary arteries, it may be more or less perfused by the LAD or the LCx. In case of occlusion of a large first diagonal branch, part of segment 12 will be involved.[101]

In our preliminary study of six patients with proximal LAD occlusion to be discussed more in detail later, either LGE or pathological SWT was assessed in segment 12 in 5/6 of the patients. The corresponding numbers for segments 15 and 16 were 6/6 and 5/6, respectively. Our preliminary observations seem to support the findings from the larger studies by Ortiz-Pérez and Setser.[96,98] Ubachs et al. analyzed 12-lead ECGs combined with SPECT imaging within 3 hours after primary PCI, and CMR of the LV within 24 hours in 11 patients with acute STEMI.[8] They found that the angiographic culprit artery was correctly designated in 91%, 82%, and 91% of cases with perfusion SPECT, CMR, and 12-lead ECG, respectively. CMR wall thickening proved to be an accurate method to localize myocardium at risk. The authors used the 12-segment polar plot system for localization of regional changes, and therefore exact comparison with the 17-segment model is not possible.

ECG and CMR Correlation

The correlation between the distribution of ST elevations in the 12-lead ECG and the myocardial AAR in CMR has not been well established. Ortiz-Pérez et al. presented the correlation between ECG leads with ST elevation and LV segments with hyperenhancement on CMR imaging.[96] As previously mentioned, with regard to the culprit artery, segments 12 and 16 showed the maximal discordance from the 17-segment model. In the patients with LGE of segment 12, 60% had ST elevation in lead I and 65% in lead aVL. In the precordial leads, the corresponding prevalence of ST elevation was less than 40% (highest prevalence in lead V_2: 37%). Regarding segment 16, the numbers for leads I and aVL were identical, while the proportions of patients with precordial ST elevations were somewhat higher (maximal 46% in leads V_4 and V_5). The authors did not report on

Table 2. Distribution of ST Elevations, Q waves, and Inverted T Waves in the 12-Lead ECG at Admission, at the Day of Cardiac Magnetic Resonance Imaging, and at Discharge in the Six Patients, a Positive Finding Refers to at Least One Affected Lead

	Admission ECG	MRI ECG	Discharge ECG
ST Elevation	**n**	**N**	**n**
I/AVL	4	2	2
V_1/V_2	6	5	4
V_3/V_4	6	5	4
V_5/V_6	1	1	2
Q Wave			
I/AVL	1	2	2
V_1/V_2	2	2	2
V_3/V_4	1	3	4
V_5/V_6	0	1	1
Inverted T Waves			
I/AVL	1	5	3
V_1/V_2	2	3	3
V_3/V_4	2	3	4
V_5/V_6	0	2	2

Table 3. Statistical Correlation between ST Elevations, Q Waves, and Inverted T Waves at Three Different Time Points, and Cardiac Magnetic Resonance Imaging, a Positive Finding Refers to at Least One Affected Lead

Time of ECG	Sensitivity	Specificity	PPV	NPV
Admission				
ST elevation	79	42	58	67
Q waves	24	91	73	55
T-wave inversion	15	73	36	46
MRI Day				
ST elevation	79	67	70	76
Q waves	39	82	68	58
T-wave inversion	52	58	55	54
Discharge				
ST elevation	73	77	75	74
Q waves	55	79	72	63
T-wave inversion	67	61	63	65

the prevalence of combined ST elevations in the lateral extremity and the precordial leads.

The authors of this article performed a preliminary (unpublished) study for the correlation of ECG changes in acute proximal LAD occlusions after successful primary PCI with segmental wall motion abnormalities using CMR as the golden standard in six male patients (age 40–70 years). The angiographic lesion site was proximal to the first LD branch in all patients. In four patients the culprit lesion was proximal and in two distal (#4 and 5) to the first septal branch. CMR scanning was arranged within 3 days of the primary PCI. Established criteria for cut points for Q waves, ST elevations, and T-wave inversions were used and the ECGs were recorded at admission, on the day of the CMR study, and at hospital discharge.[102] In the 16-segment bull's eye map, segments 1, 2, and 8 were considered as corresponding to ECG leads V_1/V_2, segments 7, 13, and 14 to leads V_3/V_4, segments 6 and 12 to leads I/aVL, and segments 11, 15, and 16 to leads V_5/V_6. The distribution of ECG changes in the 12-lead ECG is shown in Table 2 and the correlation with SWT changes on CMR in Table 3. In four of the six patients, regional CMR changes were observed both in segments 12 and 16. All of these patients had involvement of the lateral extremity leads I and aVL and in the precordial leads V_2 and V_3. The involvement of the other precordial leads varied. We think that our preliminary findings are in line with the observations by Ortiz-Pérez et al. both in the sense that segments 12 and 16 are involved in LAD occlusion, and that ST elevation in leads I and aVL are frequent in these cases.[96] As pointed out earlier, the AHA statement indicated these segments to be associated with LCx disease. It seems that standard models of LV segmentation can be used only partly in assessing individual myocardial segments in relation to coronary artery territories.

Meléndez-Ramírez et al. used myocardial edema on CMR when correlating the location of regional myocardial changes with the ECG, which included standard and additional leads.[103] They included 91 patients with a first STEMI with reperfusion therapy within 12 hours from symptom onset, who had a CMR study (mean 3 days after the ischemic event). The highest sensitivities for the ECG leads compared to the different segments (1–17) were: V_2 for basal anterior and anteroseptal, III and aVF for basal inferoseptal, III for basal inferior and inferolateral, V_7–V_9 for basal anterolateral, V_2 and V_3 for midanterior and anteroseptal, III and aVF for midinferoseptal, inferior, and inferolateral, V_2 and V_8 for midanterolateral, V_2–V_4 for apical anterior and septal, II, III, and aVF for apical inferior and lateral, and V_2–V_4 for apex. For these associations there is fairly good correlation with previously published data,[96] but for the somewhat controversial segments 12 and 16 the results differ. In the study by Meléndez-Ramirez,[103] the most

sensitive leads for segment 12 and 16 were V_2 and V_8 and I, III, and aVF, respectively, while I and aVL were the most frequently involved leads in the study by Ortiz-Pérez. Actually, in the latter study, leads II, III, and aVF were involved in only 5–10% of the cases when segment 16 showed CMR changes.[96]

The different CMR techniques used may explain some of the differences, but it is obvious that especially segments 12 and 16 remain controversial. We conclude that the main explanation for differences in different studies is that no consensus can be made about the exact borders of each vascular territory. There is an important overlap in myocardial blood supply at the anterolateral region between LAD and LCx territories concerning these controversial segments.

New Terminology for the LV Walls and Location of Q-Wave MI

The correlation between Q waves in various ECG leads and the affected myocardium has been studied by CMR. Based on these findings, a new terminology for LV walls and location of Q-wave MIs based on CMR was proposed.[99,100] A main division into the anteroseptal and inferolateral zones with subdivisions were recommended (Fig. 3). The term midanterior was recommended for MIs located especially in the midlow segments (7 and 13) of the anterior wall. This MI subtype is typically caused by occlusion of the first LD branch, and in the ECG Q waves are present in leads aVL (I) and sometimes V_2. This coincides with the previously published paper on that by Sclarovsky et al., and is also supported by the paper of Meléndez-Ramirez et al. showing that leads I and V_2 were among the most sensitive ECG leads to detect involvement of segments 12 and 16, typical for first diagonal branch occlusion in STEMI patients.[103,104]

The term true posterior MI was introduced by Grant and Murray to refer to the basal part of the LV wall positioned on the diaphragm.[105] In 1964, Perloff defined the criteria for this clinical entity as the presence of an R/S ratio of >1 and an R-wave duration >40 ms in lead V_1.[22] Later on, the term inferoposterior wall was introduced to refer to the entire wall that lies on the diaphragm. A working group statement, in agreement with the terminology of Cerqueira et al., recommended that the term posterior be abandoned and that the term inferior should be applied to the entire wall that lies on the diaphragm.[99] The recommendation was based on findings from CMR imaging, which showed that infarction of the basal and midsegments (4 and 10) of the inferior wall will generate increased R waves in leads V_3 and V_4 instead of in leads V_1 and V_2.[106] It was also shown that an infarction located in the lateral LV wall, involving more than the basal segments (segments 5 and 11), may generate increased R waves in leads V_1 and V_2. The working group recommended using the term lateral infarction in case of high R waves in leads V_1 and V_2.[99]

The observations by Bayés de Luna et al. were supported by two later studies. Van der Weg et al. evaluated the ECG in the identification and quantification of lateral wall involvement in nonanterior MI.[107] The CMR study was done 5 (2–12) days after an AMI. Significant correlations were found between lateral LV wall involvement and R waves in lead V_1 and V_6: tall and broad R waves in lead V_1 reflected lateral wall MI, especially in LCx occlusions.[107] In patients with LCx occlusion (n = 11), there was a strong correlation between the height, width, and surface of R waves in lead V_1. The surface of R waves in V_1 had the highest correlations with the apical inferior (15) and apical lateral (16) segments. Loss of height of the R wave in V_6 was found to be a sign of lateral MI, and Q waves in V_6 were related to inferolateral involvement. Also the study of Rovai et al. with 50 patients in the post-MI phase showed that a prominent R wave in lead V_1 is a specific sign of a large and transmural lateral MI.[107]

The fact that van der Weg et al. found a clear association between LCx occlusions and involvement of segment 16 may seem contradictory to the observations by Ortiz-Pérez and others discussed earlier.[96,106] However, it is clear that anatomic variation exists with respect to which coronary artery branches irrigate the apical lateral wall. In the paper of Van der Weg et al., the lateral wall included all segments of the lateral zone. Also routine clinical practice shows that there is large variation between individuals in the distribution of side branches to this area, which can be subtended by a distal LD branch from the LAD, from the intermediate artery or from branches of the LCx.

We conclude that there is no doubt that the posterior wall does not exist and that the presence of a prominent R wave in V_1 is due to lateral and not to inferior wall (especially basal) involvement.

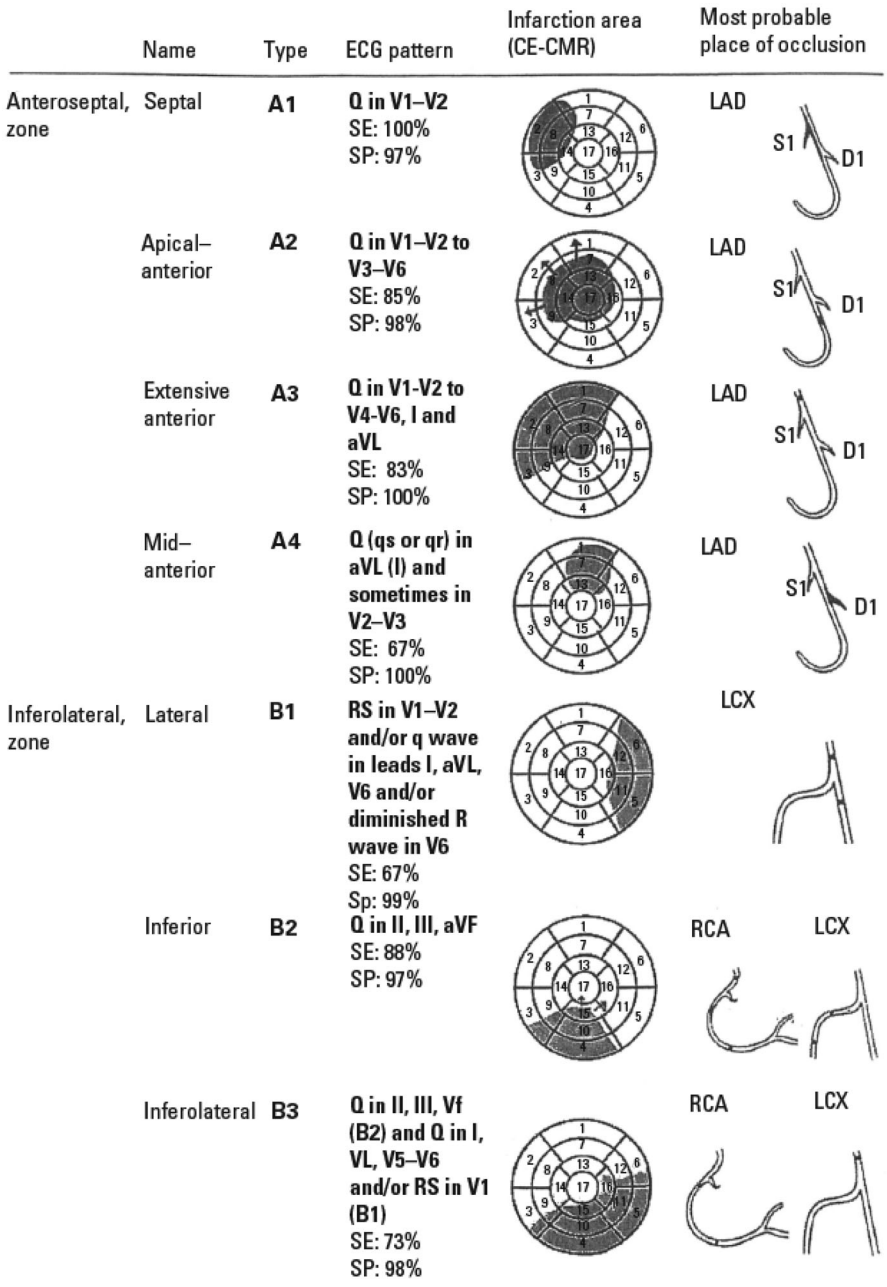

Figure 3. The new terminology for LV walls and location of Q-wave MIs based on CMR study (LV, left ventricle; MI, myocardial infarction; CMR, cardiac magnetic resonance).

CONCLUSION

CMR imaging has offered new insights into the diagnostics of cardiac diseases, including acute myocardial ischemia and infarction. Certain CMR applications, such as those used for the evaluation of myocardial viability, represent the most accurate clinical test, whereas other applications are helpful adjuncts to standard tests such as the ECG.

When using a multidisciplinary diagnostic approach to AMI, the knowledge about strengths and weaknesses of different modalities is of paramount importance. In addition, familiarity with the dynamic character of the disease and the

variations in coronary artery anatomy are of utmost importance.

Findings from studies dealing with the ECG–MRI correlation in the chronic MI phase have already resulted in changes of some basic concepts. There is general agreement that the "posterior" wall does not exist more; it is the inferobasal segment of the inferior wall. Also there is agreement that a prominent R wave in V_1 in post-MI patients is explained by a lateral wall MI. Therefore, there has not only been a change of terminology (posterior vs lateral wall), but a change of MI location (lateral wall, not the inferobasal segment of the inferior wall), and this may have several clinical implications (infarct size, presence of ventricular arrhythmia, risk for sudden cardiac death, and cardiac rupture).

Some limitations still exist. Comparing ECG and CMR findings of acute myocardial ischemia, the best agreement has been reached for the anatomic territory of the LAD, which clearly involves the segments 2, 7, 8, and 13. Regarding segments 12 and 16, which also have been ascribed to the LAD territory, there are controversial findings in the literature. In addition, no segments are 100% specific for LCx or RCA occlusion. At this moment, no all-encompassing correlation can be found between ECG and CMR findings in acute ischemia with respect to coronary anatomy. When assessing CMR findings in coronary artery disease, one has to take into consideration the variability in coronary artery anatomy.

Acknowledgment: *The authors want to express their gratitude to Ms Laura Julkunen for the help with Figure 1.*

REFERENCES

1. Keenan NG, Pennell DJ. CMR of ventricular function. Echocardiography 2007;24:185–193.
2. Plein S, Ridgway JP, Jones TR, et al. Coronary artery disease: Assessment with a comprehensive MR imaging protocol—Initial results. Radiology 2002;225:300–307.
3. Misko J, Dziuk M, Skrobowska E, et al. Co-registration of cardiac MRI and rest gated SPECT in the assessment of myocardial perfusion, function and viability. J Cardiovasc Magn Reson 2006;8:389–397.
4. Wagner A, Mahrholdt H, Holly TA, et al. Contrast-enhanced MRI and routine single photon emission computed tomography (SPECT) perfusion imaging for detection of subendocardial myocardial infarcts: An imaging study. Lancet 2003; 361:374–379.
5. Wu E, Judd RM, Vargas JD, et al. Visualization of presence, location, and transmural extent of healed Q-wave and non-Q-wave myocardial infarction. Lancet 2001;357:21–28.
6. Kim RJ, Albert TS, Wible JH, et al. Performance of delayed-enhancement magnetic resonance imaging with gadoversetamide contrast for the detection and assessment of myocardial infarction: An international, multicenter, double-blinded, randomized trial. Circulation 2008;117:629–637.
7. Ricciardi MJ, Wu E, Davidson CJ, et al. Visualization of discrete microinfarction after percutaneous coronary intervention associated with mild creatine kinase-MB elevation. Circulation 2001;103:2780–2783.
8. Ubachs FA, Engblom H, Hedström E, et al. Location of myocardium at risk in patients with first-time ST-elevation infarction: Comparison among single photon emission computed tomography, magnetic resonance imaging, and electrocardiography. J Electrocardiol 2009;42:198–203.
9. Gibbons RJ, Valeti US, Araoz PA, et al. The quantification of infarct size. J Am Coll Cardiol 2004;44:1533–1542.
10. Aldrich HR, Hindman NB, Hinohara T, et al. Identification of the optimal electrocardiographic leads for detecting acute epicardial injury in acute myocardial infarction. Am J Cardiol 1987;59:20–23.
11. Nikus K, Pahlm O, Wagner G, et al. Electrocardiographic classification of acute coronary syndromes: A review by a committee of the International Society for Holter and Non-Invasive Electrocardiology. J Electrocardiol 2010;43:91–103.
12. Aldrich HR, Wagner NB, Boswick J, et al. Use of initial ST-segment deviation for prediction of final electrocardiographic size of acute myocardial infarcts. Am J Cardiol 1988;61:749–753.
13. Birnbaum Y, Drew B. The electrocardiogram in ST elevation acute myocardial infarction: Correlation with coronary anatomy and prognosis. Postgrad Med J 2003;79:490–504.
14. Christian TF, Gibbons RJ, Clements IP, et al. Estimates of myocardium at risk and collateral flow in acute myocardial infarction using electrocardiographic indexes with comparison to radionuclide and angiographic measures. J Am Coll Cardiol 1995;26:388–393.
15. The BARI protocol. Protocol for the bypass angioplasty revascularization investigation. Circulation 1991;84 (Suppl V): V-1–V27.
16. Bartúnek J, Sys SU, Heyndrickx GR, et al. Quantitative coronary angiography in predicting functional significance of stenoses in an unselected patient cohort. J Am Coll Cardiol 1995;26:328–334.
17. Graham MM, Faris PD, Ghali WA, et al. Validation of three myocardial jeopardy scores in a population-based cardiac catheterization cohort. Am Heart J 2001;142:254–261.
18. Ortiz-Perez JT, Meyers SN, Lee DC, et al. Angiographic estimates of myocardium at risk during acute myocardial infarction: Validation study using cardiac magnetic resonance imaging. Eur Heart J 2007;28:1750–1758.
19. Levine SA, Rosenbaum FF. Prognostic value of various clinical and electrocardiographic features of acute myocardial infarction: II. Ultimate prognosis. Arch Int Med 1941:68:1215–1231.
20. Myers GB, Klein HA, Hiratzka T. Correlation of electrocardiographic and pathologic findings in large anterolateral infarcts. Am Heart J. 1948;36:838–881.
21. Surawicz B, Uhley H, Borun R, et al. The quest for optimal electrocardiography. Tast Force I: Standardization of terminology and interpretation.Am J Cardiol. 1978;41:130–45.
22. Perloff JK. The recognition of strictly posterior myocardial infarction by conventional scalar electrocardiography. Circulation 1964;30:706–718.

23. Raunio H, Rissanen V, Romppanen T, et al. Changes in the QRS complex and ST segment in transmural and subendocardial myocardial infarctions. A clinicopathologic study. Am Heart J 1979;98:176–184.
24. Moon JC, de Arenaza DP, Elkington AG, et al. The pathologic basis of Q-wave and non-Q-wave myocardial infarction: A cardiovascular magnetic resonance study. J Am Coll Cardiol 2004;44:554–560.
25. Saphir O, Priest WS, Hamburger WW, et al. Coronary arteriosclerosis, coronary thrombosis, and the resulting myocardial changes. Am Heart J 1935;10:762–792.
26. Proudfit WL, Shirey EK, Sones FM JR: Selective cine coronary arteriography: Correlation with clinical findings in 1000 patients. Circulation 1966;33: 901–910.
27. Cerqueira MD, Weissman NJ, Dilsizian V, et al. Standardized myocardial segmentation and nomenclature for tomographic imaging of the heart. A statement for healthcare professionals from cardiac imaging committee of the council on clinical radiology of the American Heart Association. Circulation 2002;105:539–542.
28. Reimer KA, Lowe JE, Rasmussen MM, et al. The wavefront phenomenon of ischemic cell death. 1. Myocardial infarct size vs duration of coronary occlusion in dogs. Circulation 1977;56:786–794.
29. Rajiah P, Desai MY, Kwon D, et al. MR imaging of myocardial infarction. Radiographics 2013;33:1383–1412.
30. Carlsson M, Ubachs JFA, Hedström E, et al. Myocardium at risk after acute infarction in humans on cardiac magnetic resonance. J Am Coll Cardiol: Cardiovasc Imag 2009;2:569–576.
31. Abdel-Aty H, Cocker M, Meek C, et al. Edema as a very early marker for acute myocardial ischemia: A cardiovascular magnetic resonance study. J Am Coll Cardiol 2009;53:1194–1201.
32. Nilsson JC, Nielsen G, Groenning BA, et al. Sustained postinfarction myocardial oedema in humans visualised by magnetic resonance imaging. Heart 2001;85:639–642.
33. Ubachs JFA, Sörensson P, Engblom H, et al. Myocardium at risk by magnetic resonance imaging: Head-to-head comparison of T2-weighted imaging and contrast-enhanced steady-state free precession. Eur Heart J Cardiovasc Imaging 2012;13:1008–1015.
34. Romagnoli A, Sperandio M, Di Roma M, et al. Anatomical and functional evaluation of the myocardium in patients with acute coronary syndrome (NSTEMI) using MR imaging. Radiol Med 2011;116:163–177.
35. Mc Namara MT, Higgins CB, Ehman RL, et al. Acute myocardial ischemia: Magnetic resonance contrast enhancement with gadolinium-DTPA. Radiology 1984;153:157–163.
36. Simonetti OP, Kim RJ, Fieno DS, et al. An improved MR imaging technique for the visualization of myocardial infarction. Radiology 2001;218:215–223.
37. Ibrahim T, Nekolla SG, Hornke M, et al. Quantitative measurement of infarct size by contrast-enhanced magnetic resonance imaging early after acute myocardial infarction: Comparison with single-photon emission tomography using Tc99m-sestamibi. J Am Coll Cardiol 2005;45:544–552.
38. Oshinski JN, Yang Z, Jones JR, et al. Imaging time after Gd-DTPA injection is critical in using delayed enhancement to determine infarct size accurately with magnetic resonance imaging. Circulation 2001;104:2838–2842.
39. Ibrahim T, Hackl T, Nekolla SG, et al. Acute myocardial infarction: Serial cardiac MR imaging shows a decrease in delayed enhancement of the myocardium during the 1st weel after reperfusion. Radiology 2010;254:88–97.
40. Engblom H, Hedström E, Heiberg E, et al. Rapid initial reduction of hyperenhanced myocardium after reperfused first myocardial infarction suggests recovery of the peri-infarction zone: One-year follow-up by MRI. Circ Cardiovasc Imaging 2009;2:47–55.
41. Saeed M, Lund G, Wendland MF, et al. Magnetic resonance characterization of the peri-infarction zone of reperfused myocardial infarction with necrosis-specific and extracellular nonspecific contrast media. Circulation 2001;103:871–876.
42. Fieno DS, Kim RJ, Chen EL, et al. Contrast-enhanced magnetic resonance imaging of myocardium at risk: Distinction between reversible and irreversible injury throughout infarct healing. J Am Coll Cardiol 2000;36:1985–1991.
43. Wong TC, Piehler K, Puntil KS, et al. Effectiveness of late gadolinium enhancement to improve outcomes prediction in patients referred for cardiovascular magnetic resonance after echocardiography. J Cardiovasc Magn Reson 2013;15:6.
44. De Waha S, Desch S, Eitel I, et al. Impact of early vs late microvascular obstruction assessed by magnetic resonance imaging on long-term outcome after ST-elevation myocardial infarction: A comparison with traditional prognostic markers. Eur Heart J 2010;31:2660–2668.
45. Scholz TD, Fleagle SR, Burns TL, et al. Nuclear magnetic resonance relaxometry of the normal heart: Relationship between collagen content and relaxation times of the four chambers. Magn Reson Imaging 1989;7:643–648.
46. Messroghli DR, Niendorf T, Schulz-Menger J, et al. T1 mapping in patients with acute myocardial infarction. J Cardiovasc Magn Reson 2003;5:353–359.
47. Moon JC, Messroghli DR, Kellman P, et al. Myocardial T1 mapping and extracellular volume quantification: A society for cardiovascular magnetic resonance (SCMR) and CMR working group of the European society of cardiology consensus statement. J Cardiovasc Magn Reson 2013;15:92.
48. Bull S, White SK, Piechnik SK, et al. Human non-contrast T1 values and correlation with histology in diffuse fibrosis. Heart 2013;99:932–937.
49. Sado DM, White SK, Piechnik SK, et al. Identification and assessment of Anderson-Fabry disease by cardiovascular magnetic resonance non-contrast myocardial T1 mapping. Circ Cardiovasc Imaging 2013;6:392–398.
50. Pedersen SF, Thrysoe SA, Robich MP, et al. Assessment of intramyocardial hemorrhage by T1-weighted cardiovascular magnetic resonance in reperfused acute myocardial infarction. J Cardiovasc Magn Reson 2012;14:59.
51. Wong TC, Piehler K, Meier CG, et al. Association between extracellular matrix expansion quantified by cardiovascular magnetic resonance and short-term mortality. Circulation 2012;126:1206–1216.
52. Kellman P, Wilson JR, Xue H, et al. Extracellular volume fraction mapping in the myocardium, Part 2: Initial clinical experience. J Cardiovasc Magn Reson 2012;14:1–8.
53. Ugander M, Oki AJ, Hsu LY, et al. Extracellular volume imaging by magnetic resonance imaging provides insights unto overt and sub-clinical myocardial pathology. Eur Heart J 2012;33:1268–1278.
54. Lockie T, Nagel E, Redwood S, et al. Use of cardiovascular magnetic resonance imaging in acute coronary syndromes. Circulation 2009;119:1671–1681.
55. Moens AL, Claeys M, Timmermans JP, et al. Myocardial ischemia/ reperfusion-injury, a clinical view on a complex pathophysiological process. Int J Cardiol 2005;100:179–190.
56. Infusino F, Niccoli G, Fracassi F, et al. The central role of conventional 12-lead ECG for the assessment of microvascular obstruction after percutaneous myocardial revascularization. J Electrocardiol 2014;47:45–51.

57. Rochitte CE, Lima JAC, Bluemke DA, et al. Magnitude and time course of microvascular obstruction and tissue injury after acute myocardial infarction. Circulation 1998; 98:1006–1014.
58. Wu KC, Kim RK, Bluemke DA, et al. Quantification and time course of microvascular obstruction by contrast-enhanced echocardiography and magnetic resonance imaging following acute myocardial infarction and reperfusion. J Am Coll Cardiol 1998;32:1756–1764.
59. Nijveldt R, Beek AM, Hirsch A, et al. Functional recovery after acute myocardial infarction: Comparison between angiography, electrocardiography, and cardiovascular magnetic resonance measures of microvascular injury. J Am Coll Cardiol 2008;52:181–189.
60. Basso C, Thiene G. The pathophysiology of myocardial reperfusion: A pathologist's perspective. Heart 2006;92:1559–1562.
61. Basso C, Corbetti F, Silva C, et al. Morphologic validation of reperfused hemorrhagic myocardial infarction by cardiovascular magnetic resonance. Am J Cardiol 2007;100:1322–1327.
62. Ganame J, Messalli G, Dymarkowski S, et al. Impact of myocardial haemorrhage on left ventricular function and remodelling in patients with reperfused acute myocardial infarction. Eur Heart J 2009;30:1440–1449.
63. Morishima I, Sone T, Okumura K, et al. Angiographic no-reflow phenomenon as a predictor of adverse long-term outcome in patients treated with percutaneous transluminal coronary angioplasty for first acute myocardial infarction. J Am Coll Cardiol 2000;36:1202–1209.
64. Mather AN, Fairbairn TA, Ball SG, et al. Reperfusion heaemorrhage as determined by cardiovascular MRI is a predictor of adverse left ventricular remodelling and markers of late arrhytmic risk. Heart 2011;97:453–459.
65. Mann DL, Bristow MR. Mechanisms and models in heart failure: The biomechanical model and beyond. Circulation 2005;111:2837–2849.
66. Sutton MGSJ, Sharpe N. Left ventricular remodeling after myocardial infarction: Pathophysiology and therapy. Circulation 2000;101:2981–2988.
67. Bax JJ, Bleeker GB, Marwick TH, et al. Left ventricular dyssynchrony predicts response and prognosis after cardiac resynchronization therapy. J Am Coll Cardiol 2004;44:1834–1840.
68. Bolli R. Mechanism of myocardial "stunning". Circulation 1990;82:723–738.
69. Choi KM, Kim RJ, Gubernikoff G, et al. Transmural extent of acute myocardial infarction predicts long-term improvement in contractile function. Circulation 2001;104:1101–1107.
70. Nowosielski M, Schocke M, Mayr A, et al. Comparison of wall thickening and ejection fraction by cardiovascular magnetic resonance and echocardiography in acute myocardial infarction. J Cardiovasc Magn Reson 2009;11: 22–32.
71. Bellenger NG, Burgess MI, Ray SG, et al. Comparison of left ventricular ejection fraction and volumes in heart failure by echocardiography, radionuclide ventriculography and cardiovascular magnetic resonance. Are they interchangeable? Eur Heart J 2000;21:1387–1396.
72. Sechtem U, Pflugfelder PW, Gould RG, et al. Measurements of right and left ventricular volumes in healthy individuals with cine MR imaging. Radiology 1987;167:425–430.
73. Masci PG, Dymarkowski S, Rademakers FE, et al. Determination of regional ejection fraction in patients with myocardial infarction by using merged late gadolinium enhancement and cine MR: Feasibility study. Radiology 2009;250:50–60.
74. Bogaert J, Bosmans H, Maes A, et al. Remote myocardial dysfunction after acute anterior myocardial infarction: Impact of left ventricular shape on regional function: A magnetic resonance myocardial tagging study. J Am Coll Cardiol 2000;35:1525–1534.
75. Rutz AK, Ryf S, Plein S, et al. Accelerated whole-heart 3D-CSPAM for myocardial motion qualification. Magn Reson Med 2008;59:755–763.
76. Götte M, Germans T, Russel IK, et al. Myocardial strain and torsion quantified by cardiovascular magnetic resonance tissue tagging: studies in normal and impaired left ventricular function. J Am Coll Cardiol 2006;48:2002–2011.
77. Zerhouni EA, Parish DM, Rogers WJ, et al. Human heart: Tagging with MR imaging—A method for noninvasive assessment of myocardial motion. Radiology 1988; 169: 59–63.
78. Axel L, Dougherty L. Heart wall motion: Improved method of spatial modulation of magnetization for MR imaging. Radiology 1989;172:349–350.
79. Sayad DE, Willet DL, Bridges WH, et al. Noninvasive quantitation of left ventricular wall thickening using cine magnetic resonance imaging with myocardial tagging. Am J Cardiol 1995;76:985–989.
80. Spotnitz HM. Macro design, structure, and mechanics of the left ventricle. J Thorac Cardiovasc Surg 2000;119:1053–1077.
81. Götte MJW, van Rossum AC, Twisk JWR, et al. Quantification of regional contractile function after infarction: Strain analysis superior to wall thickening analysis in discriminating infarct from remote myocardium. J Am Coll Cardiol 2001;37:808–817.
82. Friedrich MG, Abdel-Aty H, Taylor A, et al. The salvaged area at risk in reperfused acute myocardial infarction as visualized by cardiovascular magnetic resonance. J Am Coll Cardiol 2008;51:1581–1587.
83. Pflugfelder PW, Wisenberg G, Prato FS, et al. Serial imaging of canine myocardial infarction by in vivo nuclear magnetic resonance. J Am Coll Cardiol 1986;7:843–849.
84. Patel MR, Westerhout CM, Granger CB, et al. Aborted myocardial infarction after primary percutaneous coronary intervention: Magnetic resonance imaging insights from the Assessment of Pexelizumab in Acute Myocardial Infarction (APEX-AMI) trial.Am Heart J. 2013;165:226–233.
85. Wince WB, Kim RJ. Molecular imaging: T2-weighted CMR of the area at risk: A risky business? Nat Rev Cardiol 2010;7:547–549.
86. Arai AE, Leung S, Kellman P. Controversies in cardiovascular MR imaging: Reasons why imaging myocardial T2 has clinical and pathophysiologic value in acute myocardial infarction. Radiology 256;1:23–32.
87. Matsumoto H, Matsuda T, Miyamoto K, et al. Peri-infarct zone on early contrast-enhanced CMR imaging in patients with acute myocardial infarction. J Am Coll Cardiol:Cardiovasc Imag 2011;4:610–618.
88. Arai AE. Gadolinium can depict area at risk and myocardial infarction: A double-edged sword? J Am Coll Cardiol Cardiovasc Imag 2011;4:619–621.
89. Dall'Armellina E, Piechnik SK, Ferreira VM, et al. Cardiovascular magnetic resonance by non contrast T1: Mapping allows assessment of severity of injury in acute myocardial infarction. J Cardiovasc Magn Reson 2012;14:15.
90. Ugander M, Bagi PS, Oki AJ, et al. Muyocardial edema as detected by pre-contrast T1 and T2 CMR delineates area

at risk associated with acute myocardial infarction. J Am Coll Cardiol: Cardiovasc Imag 2012;5:596–603.
91. Versteylen MO, Bekkers SCAM, Smulders MW, et al. Performance of angiographic, electrocardiographic and MRI methods to assess the area at risk in acute myocardial infarction. Heart 2012;98:109–115.
92. Wilkins ML, Pryor AD, Maynard C, et al. An electrocardiographic acuteness score for quantifying the timing of a myocardial infarction to guide decisions regarding reperfusion therapy. Am J Cardiol 1995;75:617–620.
93. Sejersten M, Ripa RS, Maynard C, et al. Timing of ischemic onset estimated from the electrocardiogram is better than historical timing for predicting outcome after reperfusion therapy for acute anterior myocardial infarction: A DANish trial in Acute Myocardial Infarction 2 (DANAMI-2) substudy. Am Heart J 2007;154:61.e1–8.
94. Pereztol-Valdés O, Candell-Riera J, Santana-Boado C, et al. Correspondence between left ventricular 17 myocardial segments and coronary arteries. Eur Heart J 2005;26:2637–2643.
95. Ortiz-Pérez JT, Rodriguez J, Meyers SN, et al. Correspondence between the 17-segment model and coronary arterial anatomy using contrast-enhanced cardiac magnetic resonance imaging. J Am Coll Cardiol: Cardiovasc Imaging 2008;1:282–1293.
96. Javadi MS, Lautamäki R, Merrill J, et al. Definition of vascular territories on myocardial perfusion images by integration with true coronary anatomy: A hybrid PET/CT analysis. J Nucl Med 2010;51:198–203.
97. Setser RM, O'Donnell TP, Smedira NG, et al. Coregistered MR imaging myocardial viability maps and multi-detector row CT coronary angiography displays for surgical revascularization planning: Initial experience. Radiology 2005; 237:465–473.
98. Bayes de Luna AB, Wagner G, Birnbaum Y, et al. A new terminology for left ventricular walls and location of myocardial infarcts that present Q wave based on the standard of cardiac magnetic resonance imaging: A statement for healthcare professionals from a committee appointed by the International Society for Holter and Noninvasive Electrocardiography. Circulation 2006;114:1755–1760.
99. Bayes de Luna A. Location of Q-wave myocardial infarction in the era of cardiac magnetic resonance imaging techniques: An update. J Electrocardiol 2007;40:69–71.
100. Donato P, Coelho P, Santos C, et al. Correspondence between left ventricular 17 myocardial segments and coronary anatomy obtained by multi-detector computed tomography: An ex vivo contribution. Surg Radiol Anat 2012;34:805–810.
101. Thygesen K, Alpert JS, White HD, et al. Universal definition of myocardial infarction. Circulation 2007;116:2634–2653.
102. Meléndez-Ramirez G, de Micheli A, Fratti V, et al. Relación entre los hallazgos electrocardiográficos y de resonancia magnética en la fase aguda del infarto miocárdico. Arch Cardiol Mex 2011;81:298–303.
103. Sclarovsky S, Birnbaum Y, Solodky A, et al. Isolated mid-anterior myocardial infarction: A special electrocardiographic sub-type of acute myocardial infarction consisting of ST-elevation in non-consecutive leads and two different morphologic types of ST-depression. Int J Cardiol 1994;46:37–47.
104. Grant RP, Murray RH. The QRS complex deformity of myocardial infarction in the human subject. Am J Med 1954;17:587–609.
105. Bayés de Luna A, Cino JM, Pujadas S, et al. Concordance of electrocardiographic patterns and healed myocardial infarction location detected by cardiovascular magnetic resonance. Am J Cardiol 2006;97:443–451.
106. van der Weg K, Bekkers S, Winkens, B, et al. Evaluation of the electrogardiogram in identifying and quantifying lateral involvement in nonanterior wall infarction using cardiovascular magnetic resonance imaging. J Electrocardiol 2012;45:478–484.
107. Rovai D, Di Bella G, Rossi G, et al. A prominent R wave in V_1 but not in V_2 is a specific sign of a large lateral transmural infarction. Rev Esp cardiol 2012;65:1101–1105.